

Stress and strain distribution in twist extrusion of AA6063 aluminum alloy

Sara Sadat Hosseini Faregh¹  · Amir Hassani¹

Received: 15 August 2016 / Accepted: 16 January 2017 / Published online: 1 March 2017
© Springer-Verlag France 2017

Abstract Twist extrusion is one of the common methods in the area of severe plastic deformation. By passing the sample through a twist channel grain refinement will occur. In this article, the twist extrusion process is modeled by ABAQUS finite element software. Three different approaches are used for prediction of strain field distribution for higher passes of TE. The FE results are compared with the experimental results of twist extruded AA6063 aluminum alloy specimens. A sensitivity analysis has been implemented to choose the proper element size and friction coefficient during simulation. The microstructures of TE samples have been observed by SEM microscopy and analyzed by Pixcaviator software. Comparing the results of the microstructure study and FE shows that importing the material properties and deformation field from the previous pass to the current pass is the best way to simulate a multi-pass twist extrusion process. The plastic strain distributions show that the effective plastic strain is higher at the corner of the samples than at the center of it. The FE results show that the maximum Von-Mises stress increases at the corner elements by increasing the extrusion passes from 42 MPa at pass #1 to 110 MPa at pass #7. Most of this increase occurs in the first three passes.

Keywords Twist extrusion (TE) · Finite element · Plastic strain · Friction coefficient

Introduction

Severe plastic deformation (SPD) processes are metal forming processes which impose a high strain field through extensive hydrostatic pressure into a bulk solid without significant changes in the overall dimension of a sample. The main advantage of such processes is generating exceptional grain refinement [1]. SPD processes can be divided into two categories: top-down methods and bottom-up methods. In top-down methods the sample is processed so that grain refinement occurs and the sample becomes strengthened. Some of the top-down SPD processes introduced by researchers include high-pressure torsion (HPT) [2], equal channel angular pressing (ECAP) [3], multi-directional forging (MDF) [4], accumulative roll-bonding (ARB) [5], repetitive corrugation and strengthening (RCS) [6], and twist extrusion (TE) [7, 8]. In bottom-up methods firstly refined grains are produced, then they are combine to manufacture an external sample. This method uses hot isostatic pressing (HIP) and spark plasma sintering (SPS) for packing of grains. Dynamic Severe Plastic Deformation (DSPD) is a secondary process after HIP that was introduced by Abdul-Latif et al. [9–11].

The twist extrusion process has been successfully employed for different materials, such as copper [8], titanium [12, 13], and aluminum [14–19]. The process manufactures long, straight semi-finished parts in the form of solid and hollow cross sections and various complexities. In the process, the billet is extruded through a die by applying hydrostatic pressure at the bottom of the sample. The die consists of a twisted channel by rotation angle α and slope angle β . The billet cross section remains constant after finishing the process [20]. There are different SPD extrusion based processes, such as twist extrusion, twist channel angular pressing [21], and planar twist extrusion [22]. In these types of processes complicated boundary conditions and complex plastic

✉ Sara Sadat Hosseini Faregh
sara_h_f@hotmail.com

¹ Department of Metallurgy and Materials Science, Semnan University, Semnan, Iran

deformation fields exist. Use of finite element analysis is a mandatory tool for prediction of stress and strain field distribution. The microstructure evolution and mechanical properties of the deformed sample are directly related to the extent of plastic deformation. Therefore, determination of stress and strain changes due to different passes of TE will help to understand the process and better predict the properties. Several studies have been carried out covering plastic deformation analyses in a twist extrusion process [8–13]. Most of them have investigated the process experimentally and detailed theoretical investigation has not been implemented until now, especially in conjunction with stress, strain, and strain rate distributions of a specimen. Varyukhin et al. [7] expressed an equation for prediction of strain in rectangular cross sections. The equation states that a square cross section will experience smaller strains than rectangular cross section with aspect ratio 1.3–1.5. Also, higher twist angle induces larger strains in each pass.

In this article, the finite element software ABAQUS is used to investigate the plastic deformation behavior of materials during twist extrusion by considering the processing conditions, such as mesh size and friction. The finite element analysis is verified by the results of experimental tests carried out by Zendehdel and Hassani [18] on AA-6063 aluminum alloy.

Materials and methods

In this section firstly the finite element modeling approach will be described then the experimental sample specifications will be introduced.

Finite element modeling

The finite element model involved extruding a billet through a die. The TE die inlet was a $15 \times 15 \text{ mm}^2$ cross section. The sample was twisted 90° clockwise. The die twisting region had 30° slope. The twist extrusion process was modeled in 3D space of Abaqus/Explicit finite element software. The dies, ram and guides were modeled as rigid parts and the billet was deformable. Analysis was carried out by the dynamic temperature–displacement (explicit) solver of the software. The nonlinear geometry was enabled to consider large deformation.

The billet and die contact surfaces were modeled with a surface to surface finite sliding contact pair algorithm. The frictional form of this algorithm was also used to model the contact surfaces between the ram and the billet. A separable contact algorithm was used for describing the die and the billet contact surfaces. A non-separable contact algorithm was used for describing the ram and the billet contact surfaces.

The applied boundary conditions were similar to the experimental tests. Therefore, the six degrees of freedom of dies

were foreclosed and the ram could move only parallel to the billet axis during the deformation. Instead of applying load or pressure into ram, the ram was forced to move 0.11 m downward to quit the billet from the die. The ram speed was equal to 6 mm/s. In this way, the force of extrusion could be predicted independent of the experimental procedure. In addition, the initial temperature of the billet was set to be equal to 298 K as the thermal boundary condition. The billet was meshed by a C3D8RT element type. This element type was a 3D, 8-node thermally coupled brick continuum element with reduced integration calculation. The die was meshed by an R3D4 element type, a 4-node 3D bilinear rigid quadrilateral element. A mesh sensitivity analysis and friction coefficient were carried out. The mesh size changed from 0.25 to 2 mm and the friction coefficient between the die and sample surface varied from 0 to 0.15. After the mesh sensitivity analysis, the mesh size 0.5 mm was selected for final simulation of different passes of TE. With this mesh size, the billet had a total of 109,330 elements and 117,900 nodes. Also, the die had 35,400 elements and 35,521 nodes.

The mechanical properties used to simulate the TE process are shown in Table 1. The elastic-plastic behavior of the sample is defined according to the tension test results. The results of the tension test have been modified to enter true stress and plastic strain as inputs of plastic behavior. After submitting the solution, the computation time varies from 4.5 h for a mesh size of 2 mm to 70 h for a 0.25 mm mesh size for each pass of extrusion. Figure 1 shows the finite element model of the TE process before and after completing the analysis.

After doing the mesh and friction coefficient sensitivity analysis, three different methods were selected for simulating the higher passes of the twisted extrusion process, as follows:

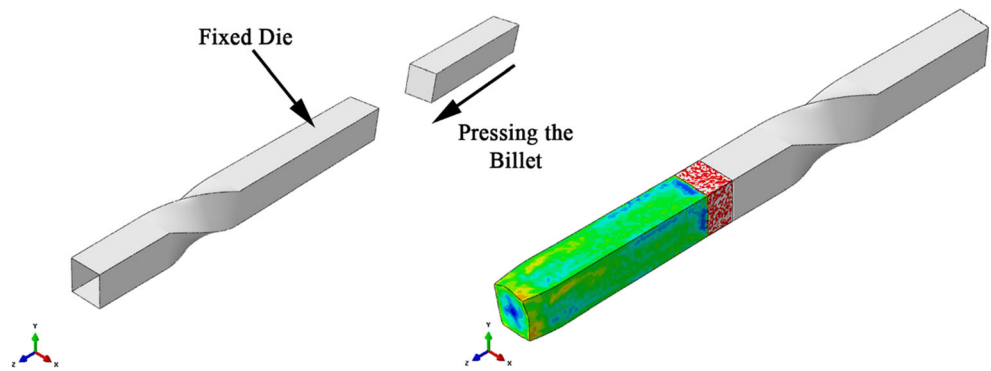
- 1- Transferring the deformation resulting from the first pass and no changes in the mechanical properties at the next pass;
- 2- Transferring changes of mechanical properties and deformation results from the previous pass to the next pass;
- 3- Transferring changes of mechanical properties without considering the deformation caused by previous pass.

In the first method the results of the tension test for the annealed sample were defined as a material property and there

Table 1 Mechanical properties of AA 6063 defined in FE software

Elastic Modulus (GPa)	70
Poisson Ratio	0.3
Density (kg/m^3)	2730
Yield Strength (MPa)	48.7
Ultimate Tensile Strength (MPa)	94.7
Maximum Strain (%)	16.8

Fig. 1 Finite element model of twist extrusion process



was no change in subsequent passes. However, in the second and third methods the plastic behavior was changed by corresponding tension test results. The results of the pass #1 tension test were entered into the property module of the software for simulating pass #2 TE. These three methods were applied in a finite element model and a proper method which is consistent with the experimental results was selected.

Materials and sample preparation

The material used in [18] was AA6063 aluminum alloy. The initial billet was in the form of extruded billet (90 mm diameter and 700 mm length). The chemical composition of the initial billet is showed in Table 2. The billet was directly extruded at 400 °C. The final form of the billet was a square rod (8.4 m length and 14.6 × 14.6 mm² cross section) [18].

The samples were cut perpendicular to the cross section and prepared for metallographic investigations. After polishing, the microstructural evolution was observed in the center and lateral edges using scanning electron microscopy (SEM). The true strain values were calculated using eq. 1.

The microstructural evolution was studied in the center and lateral edges of the TE sample’s cross section by scanning electron microscopy (SEM). The strain could be calculated according to the average grain diameter. Equation 1 shows the definition of strain according to grain diameter:

$$\epsilon = \ln\left(\frac{d_0}{d_1}\right)^2 \tag{1}$$

Where d_0 and d_1 are the average diameters of grains before and after the twist extrusion process. Beygelzimer et al. [23] derived eq. 2 for prediction of strain distribution in the TE process.

$$\epsilon(r) = \frac{2}{\sqrt{3}} \frac{r}{R} \tan\gamma \tag{2}$$

Where r is the radial distance to the center of the die, R is the maximum distance from the die center and γ is the twist angle of the die. The strain varies from the center to the lateral edge of the sample so grain refinement is different at the surface and the center of the sample. The process of grain refinement in polycrystalline materials have been studied by Beygelzimer [24].

Based on this approach, the scanned images (150 dpi) of the longitudinal cross section were analyzed by Pixcavator IA 4.3 image analysis software to determine the average grain area (μm^2) and consequently mean true strain. Pixcavator IA 4.3 software calculated the average of the grain area and then the average diameter was calculated. In the case of twinning and detwinning, this method is not appropriate. However, in the SEM images twinning or detwinning was not observed (as will be shown in Fig. 2).

Results and discussion

In this section firstly the SEM observations will be shown then the finite element modeling results will be presented, followed by a comprehensive discussion of the results.

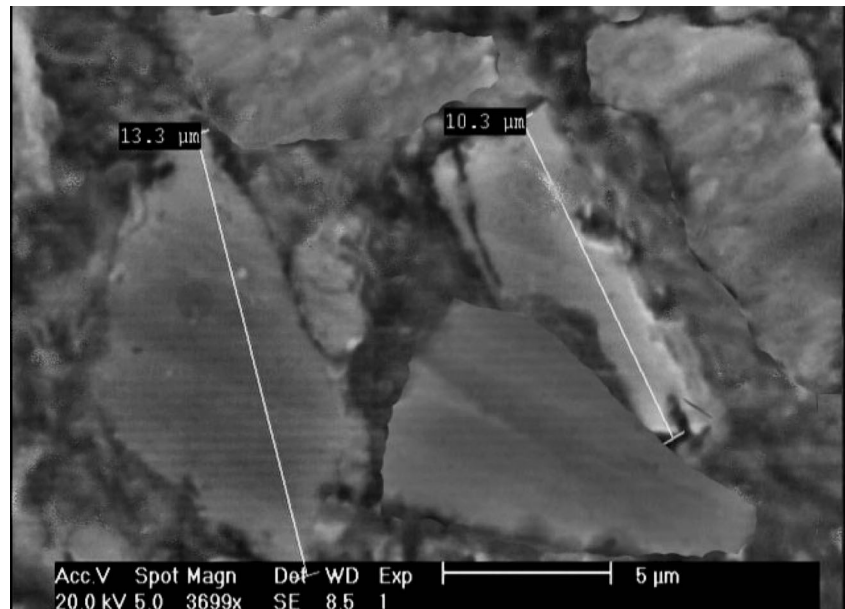
Microstructure observations

Figure 2 shows the SEM observations of the sample cross section before twist extrusion. The grains are distinctly coarse [18]. Figure 3 shows the SEM images of the sample after pass #1 of TE [18]. The microstructure of the twisted sample is different at the center and lateral edges. The

Table 2 Chemical composition of the 6063 aluminum alloy used [20]

Element	Mg	Si	Fe	Cu	Mn	Cr	Zn	Ti
Weight percent	0.707	0.585	0.350	0.084	0.100	0.020	0.110	0.038

Fig. 2 SEM image of AA 6063 microstructure of annealed sample [18]



lateral edges experience higher shear strains compared to the center of the sample, as reported previously by [25].

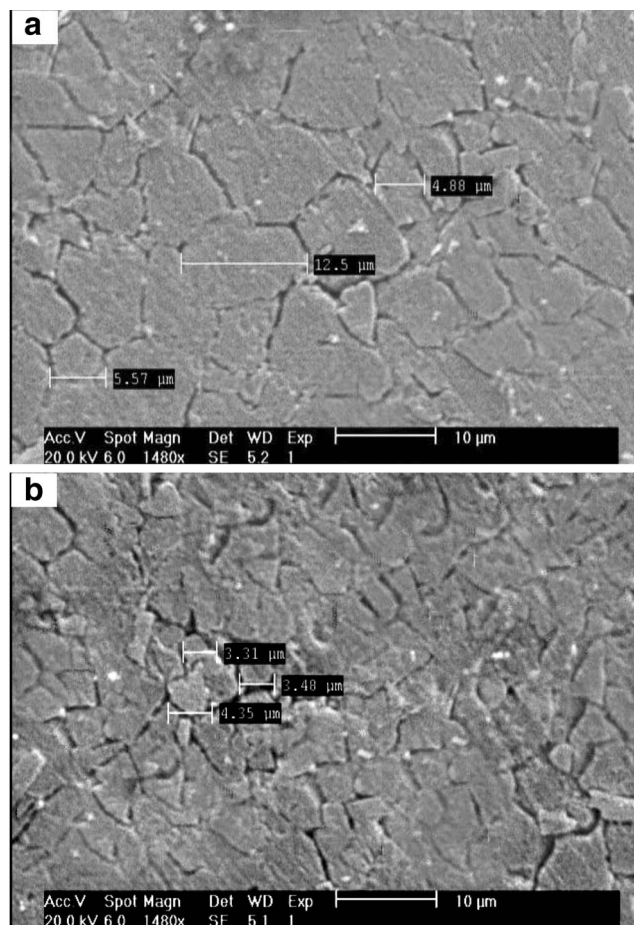


Fig. 3 SEM image of AA 6063 microstructure after pass #1 of TE (a) center of the sample, (b) lateral edge of the sample [18]

The strain value increases in a radial direction from the center of the cross section towards the edges. The true strain values can be calculated using Eq. 1 over SEM image analysis before and after the TE process. Table 3 shows the results of the image analysis for the initial sample and sample pass #1 TE. The experimental results will be used to verify the finite element analysis of the TE process.

Sensitivity analysis results

The plastic strain distributions have been used to investigate the effect of mesh size on the accuracy of results. The plastic strain distributions were extracted for the mesh sizes of 0.25, 0.5, 1, and 2 mm and compared with each other. Figure 4 shows the finite element results of the TE process for different mesh sizes.

Comparing the plastic strain distribution identifies that the mesh size of 0.5 mm provides good accuracy for the model. The simulation run time for the mesh sizes of 0.5 and 0.25 mm was 18 and 70 h (found using a 4-core computer system) respectively. Running the FE model by a mesh size of 0.5 mm is more cost effective and leads to almost the same results. Comparing the mesh sizes for

Table 3 Results of image analysis of the annealed and TE sample at the end of the pass #1

	Average area of grains (μm^2)	Generated strain
Before TE	13.143	(NA)
Center of the sample	12.433	0.0555
Lateral edge of the sample	7.951	0.5025

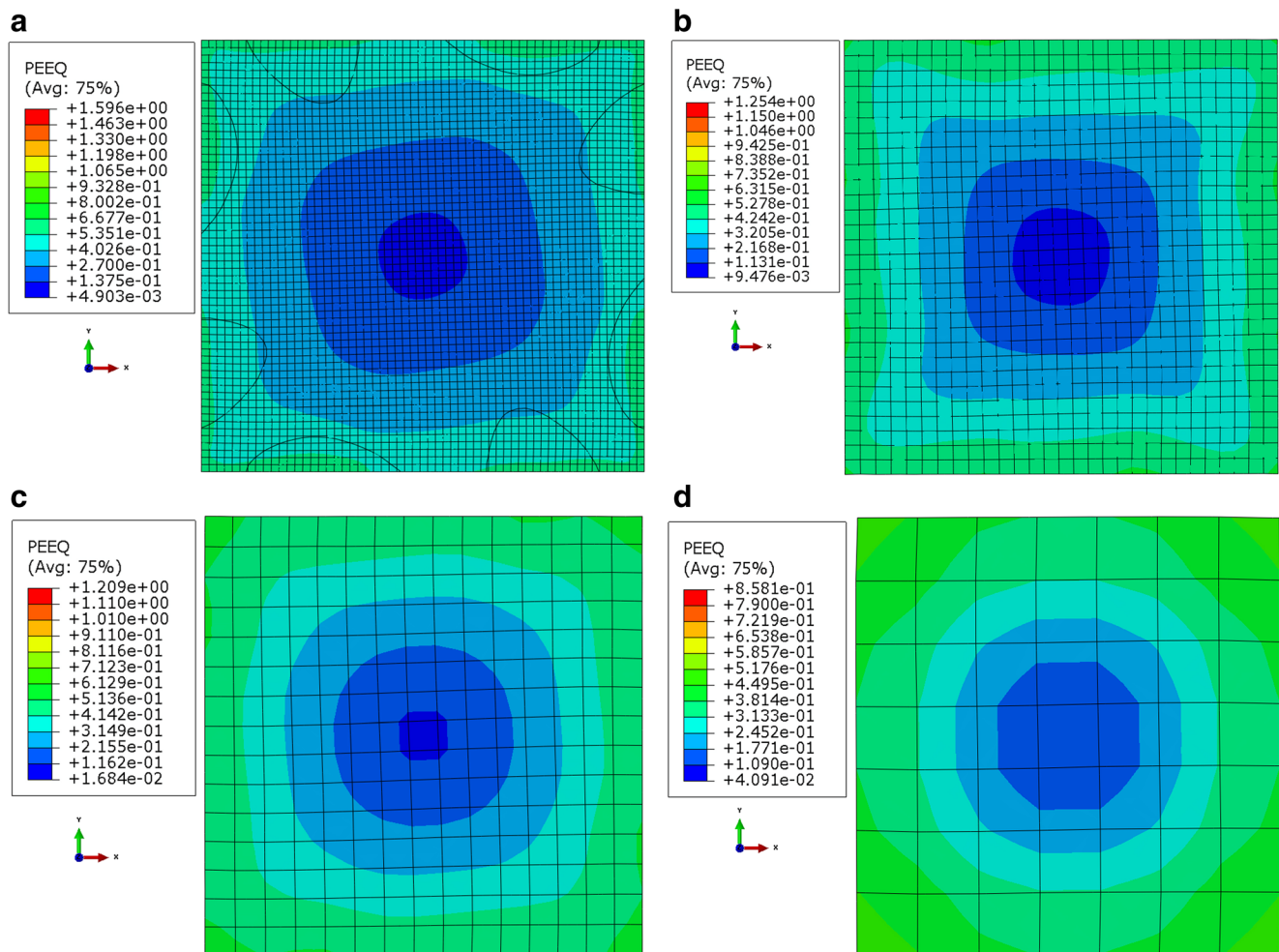


Fig. 4 Plastic strain distribution of pass #1 TE by mesh sizes of (a) 0.25, (b) 0.5, (c) 1, and (d) 2 mm

the TE process and other forming analysis [26–28] shows that a mesh size of 0.5 mm is small enough to obtain accurate results.

Figure 5 shows the plastic strain distribution for the friction coefficients of 0, 0.1, and 0.15. An increase of friction coefficient from 0 to 0.1 had no considerable effect on the strain distribution of the TE sample. Nagasekhar et al. [29] also reported that an increase in the friction coefficient leads to increasing the required load of forming. Also, Latypov et al. [30] indicated that friction plays a minor role in the die filling. Comparing the FE results for friction coefficients 0.1 to 0.15 shows a 2% increase in the strain value of the TE samples. So, changing the friction coefficient had no considerable effect on the FE results. The friction coefficient can be assumed to be constant and equal to 0.1.

Figure 6 shows the variation of Von Mises stress and plastic strain in different sections while forming the sample by the pass #1 TE process. The results are illustrated for a mesh size of 0.5 mm and friction coefficient of 0.1. The stress value was higher for the deformation region, which shows that a

considerable shear strain was produced in the sample due to the twisting in the mold. This shear stress caused about a 42 MPa increase in Von Mises stresses at the corners and consequently an increase in flow stress of the sample after pass #1 TE, as well as sample wrap at the corners.

The results of the image analysis (Table 3) determined that the plastic strain was equal to 0.5 for the lateral edges. The results of the equivalent plastic strain distribution by FE analysis (Fig. 4) predicted a similar value for pass #1 TE. The error between the experimental and FE results equals 5%. Comparing the results shows good accuracy between experimental and numerical model.

FE results for multi-pass TE

Three different methods have been introduced for multi-pass simulation of the TE process. Figure 7 shows the FE results of passes #1 and #2 using the first method. Comparison of the results shows that the stresses caused by pass #2 were not considerably different from the results of pass #1. This issue emphasizes the fact that the ABAQUS software cannot

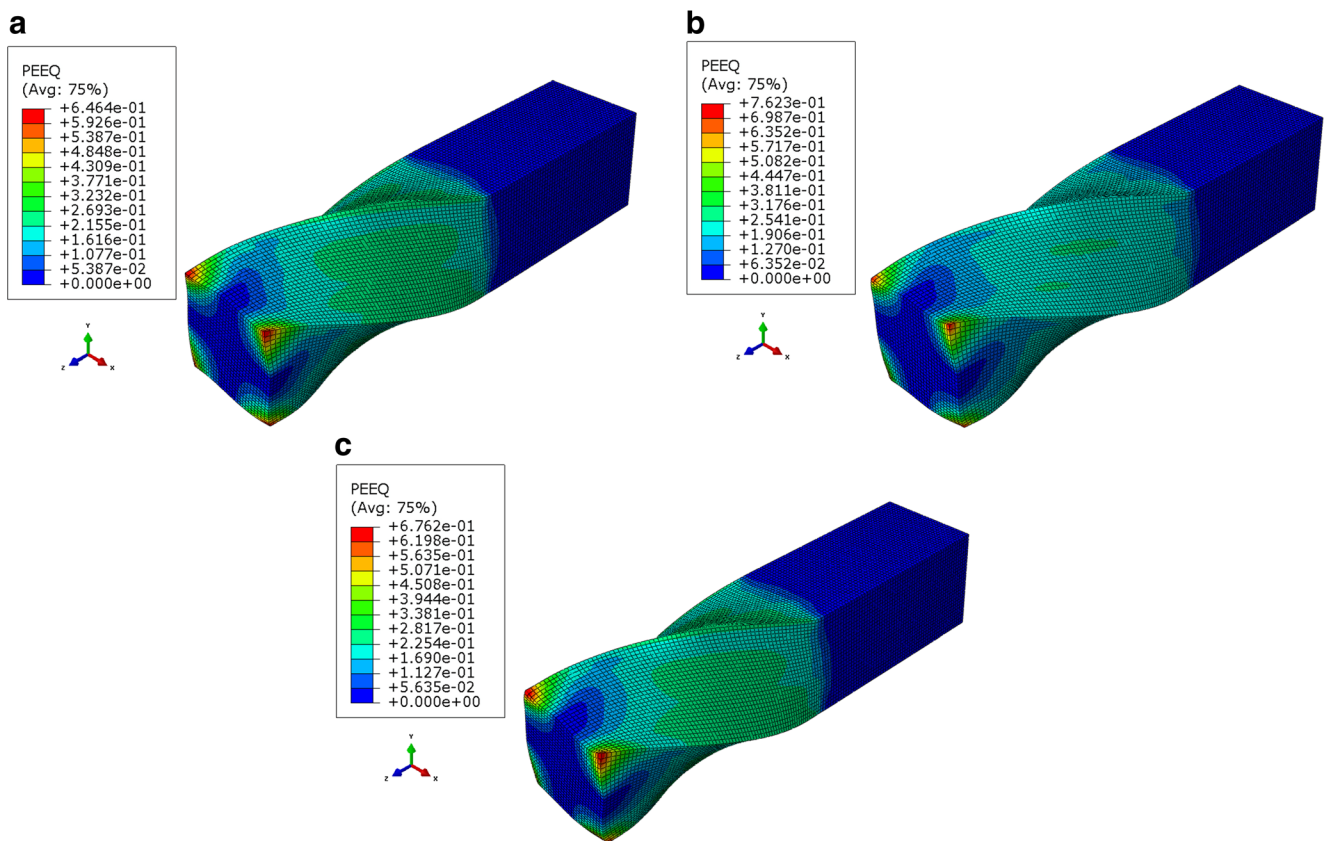


Fig. 5 Plastic strain distribution during pass #1 TE by the friction coefficient of (a) 0, (b) 0.1, and (c) 0.15

accomplish the grain refining during the TE process. For this reason, the first method is not appropriate and will not be discussed any more. To include the effect of grain refinement in finite element model, the material properties that depend on grain size have been modified in each pass and new values defined as input. In the second and third methods, this point has been applied.

In the second method of FE modeling, the induced stress and strain distribution due to the material deformation in the first pass has been transferred into the model.

Also, the material properties have been modified by entering the tension test results in the property module of the software. Figure 8 shows the distribution of plastic strain and Von Mises stress inside the twist extruded sample at the end of pass #2 TE.

The third method consisted of modifying the material properties according to the tension test results. In this method the loading history has not been imported from pass #1. Figure 9 illustrates the distribution of plastic strain and Von Mises stress at the end of the pass #2 TE.

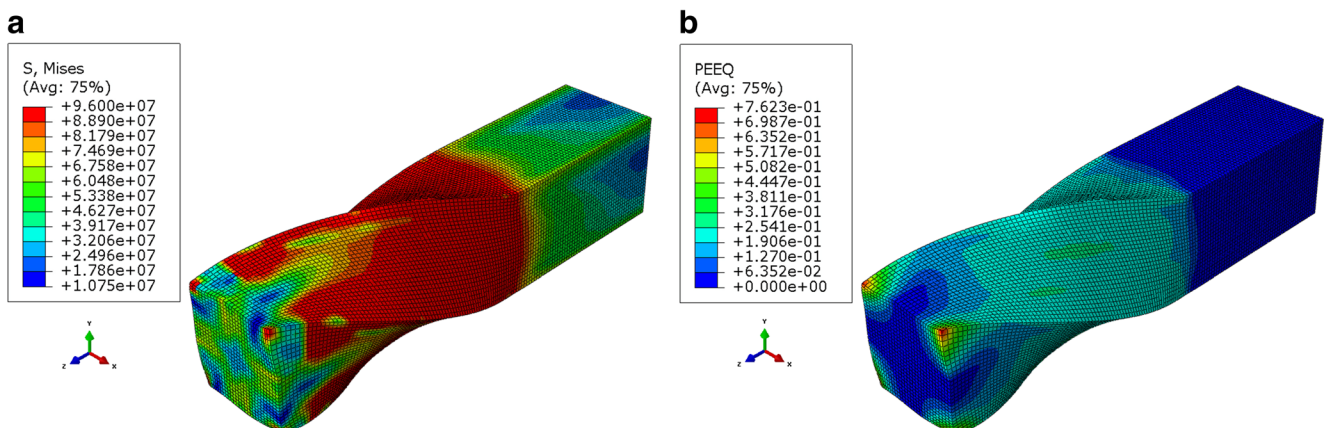


Fig. 6 Distribution of (a) stress and (b) strain during pass #1 of the TE process

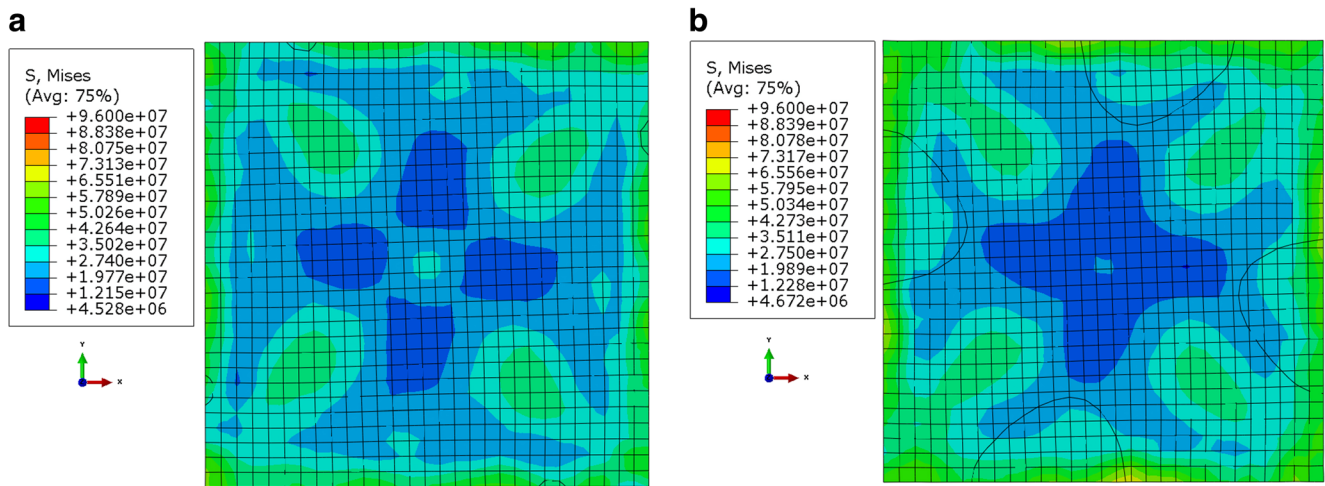


Fig. 7 Distribution of stress in (a) pass #1 and (b) path #2 TE process using the first method

Comparing the results of the pass #2 TE process using the second and third methods shows that the induced plastic strain in the sample was in an aggregated form; i.e. at each pass, a certain value was added to the plastic strain value. By modifying the material properties in pass #2, a slight increase was observed in the stress distribution. In all FE models, the shear stress helped deformation accomplishment and the twist extrusion process was performed without fracture of the sample.

After comparing the results of pass #2 TE and the introduced methods, the second approach has proved to be more consistent with the experimental results extracted from the image analysis of the TE samples. Table 4 compares the strain value at the center and lateral edges of the twist extruded samples for experimental and FE analysis. The results show that the second method can predict strain at the center and lateral edges with good precision and minimum error compared to other methods. Thus, transferring the changes of material properties and the deformation

caused by the previous pass has been selected as the proper method for modeling the multi-pass TE process.

The second approach has been used for simulation of multi-pass TE. Figure 10 shows the Von Mises stress distribution across the radial distance from the center of the cross-section of the sample for passes #1, #2, #3 and #7. The results of pass #4 to #6 set between the results of pass #3 and #7 and have not been showed in Fig. 10 for clarification. The magnitude of Von Mises stress increases continuously. The rate of increase reduces after pass #3 as it was reported previously by other researchers of SPD. The maximum magnitude of Von Mises stress occurs at corners of billet because of the contact between the interior surface of die and the billet [8, 14, 15, 18]. The maximum stress in pass #1 TE was equal to 42 MPa in the corner elements. The maximum stress equaled 60, 92, and 110 MPa for passes #1, #2, #3, and #7 respectively in the corner elements. The rate of increase in Von Mises stress reduced by increasing the number of TE passes.

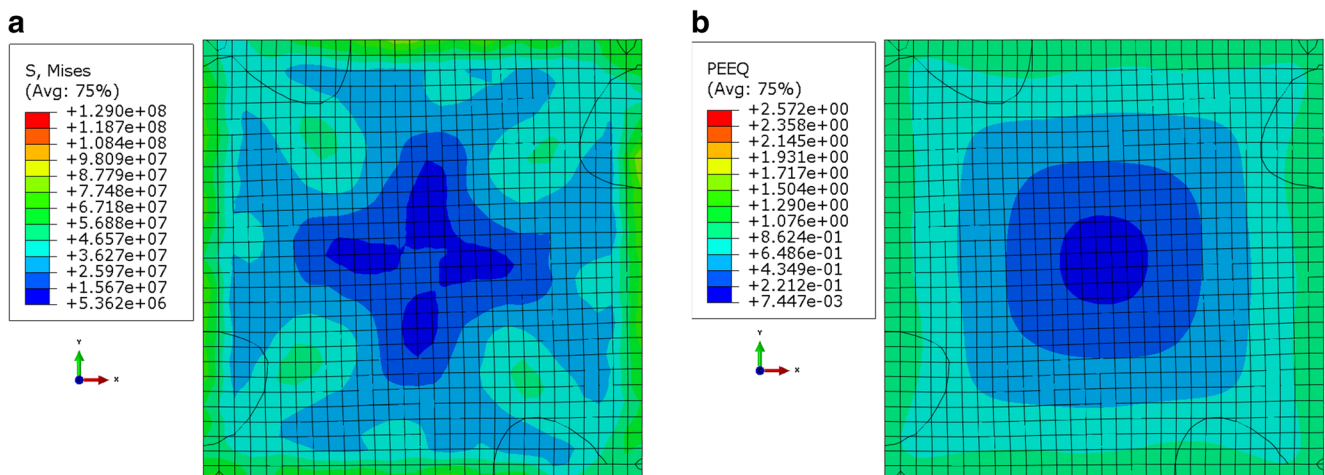


Fig. 8 Distribution of (a) stress and (b) plastic strain in pass #2 TE process using the second method

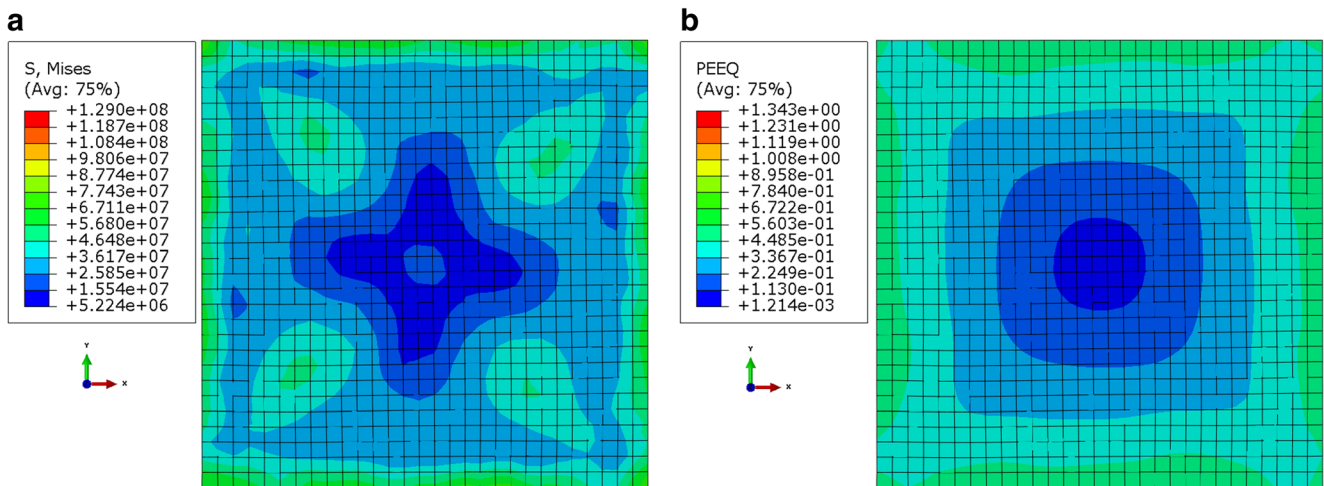


Fig. 9 Distribution of (a) stress and (b) plastic strain in pass #2 TE process using the third method

By increasing the number of passes, strain saturation occurred in the sample. Strain saturation is one of the SPD process specifications. After a certain pass, microstructures will not be changed noticeably.

Figure 11 shows the variations of the Von Mises stress during the deformation time for passes #1, #2, #3 and #7 of the TE process. Figure 12 shows the variation of plastic strain for the same passes. The stress increased at the beginning of the process. After passing the sample from the twist channel, the stress decreased. The peripheral regions of the sample were subjected to considerable shear stresses due to the friction of the die and surface of the sample.

Figure 13 shows the variation of plastic strain during deformation for the center and corner elements in the twist extruded sample. The effective strains at the center of the sample were less than the strains in the corner. The corner elements experienced larger strains due to the frictional force between the die and the sample while the center elements had lower strains, mostly because of pure shear. The results are consistent with the experiments reported in [12, 27]. The plastic strain for the multi-pass twist extrusion was calculated by eq. 1 and analysis of the SEM images.

The plastic strains obtained from the experimental results are shown in Fig. 14. Comparing the results of finite element modeling and the results obtained from the image analyses of the TE samples indicates that the expanded finite element

model can predict induced strains very well (5% difference). The grain refinement size and dependent properties can be predicted with acceptable error by determining the induced strains from the finite element results.

Figure 14 also shows the strain at the center of the die. This magnitude of strain is created due to happening of the cross flow in the TE process. Kulagin [31] investigated the cross flow of materials due to the TE. The material flow during the TE can be decomposed into a helical flow and deviations from the helical flow. The helical flow means ideal die-controlled motion of a transverse section of the billet. Deviations from the helical flow is called “cross flow” and results in planar flow within the transverse section of the billet. Due to the helical flow, each point in the transverse section preserves their relative location and move in the extrusion direction. In contrast, the cross flow leads to displacement of the points from their initial locations in the transverse planes. The cross flow during the TE

Table 4 Comparing the results of FE analysis and experimental measurement for pass #2

	Strain at center	Strain at lateral edge	Mean error percent
Experimental measurement	0.12	0.89	(NA)
FEM-second method	0.1	0.98	13
FEM-third method	0.06	0.48	48

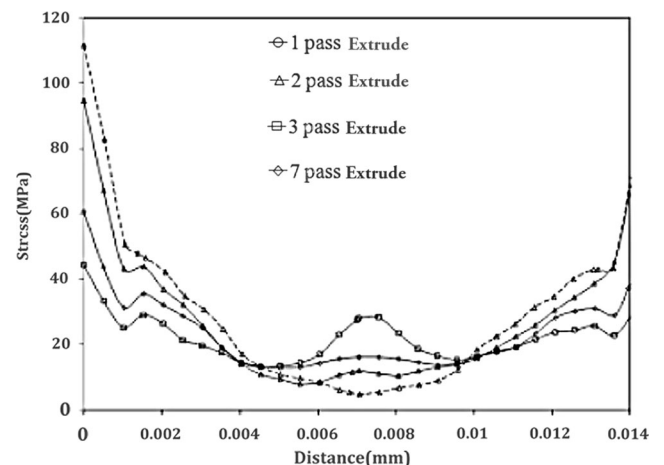


Fig. 10 Variation of the Von Mises stress distribution across the radial distance from the center of the cross-section of the sample for passes #1, #2, #3 and #7

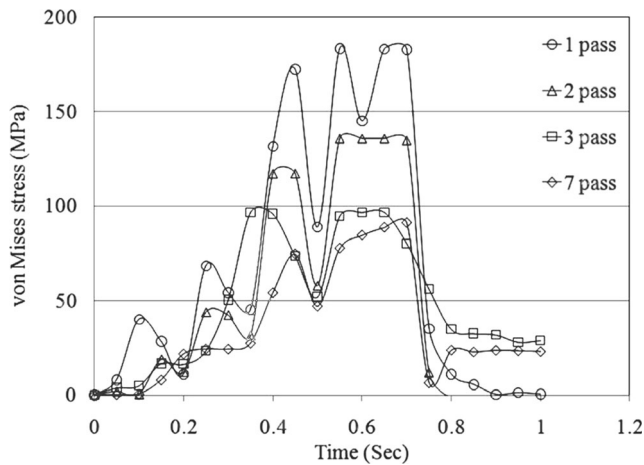


Fig. 11 Variations of the Von Mises stress during the deformation time for passes #1, #2, #3 and #7

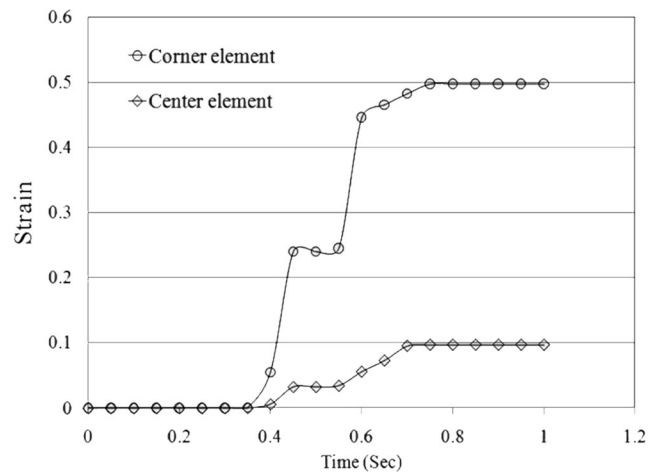


Fig. 13 Plastic strain variation at center and corner in pass #1 TE

provides nonzero strains in the vicinity of the billet center. These strains at the central region are essential for the formation of uniform ultrafine-grained microstructures. Particularly, using the TE dies with higher twist angles and smaller heights of the twist zone increases magnitudes of the cross flow. Also, the cross flow can be also intensified by increasing the friction coefficient between the die and the billet.

Conclusions

In this article, finite element analysis and experimental studies related to the twist extrusion process have been discussed. Experimental tests were carried out for AA-6063 aluminum alloy. The main findings of this research can be listed as follows:

- An increase of friction coefficient from 0 to 0.15 had no considerable effect on the plastic strain distribution of TE samples.
- Comparison of the finite element results and the results of the microstructural study obtained from image analysis shows that applying the material properties change and importing the deformations created in the previous passes of TE (second FE method) is the best method for modeling a multi-pass TE process in ABAQUS software.
- By increasing the number of passes, the rate of stress increase will be reduced so that the stress at pass #7 increases only 14% relative to pass #3. The strain saturation is the main cause of this rate reduction.
- The lateral edges of the TE sample experience higher stress and strains in comparison to the center of the sample.
- The increase in material properties is higher in the first three passes compared to the next four passes of TE.

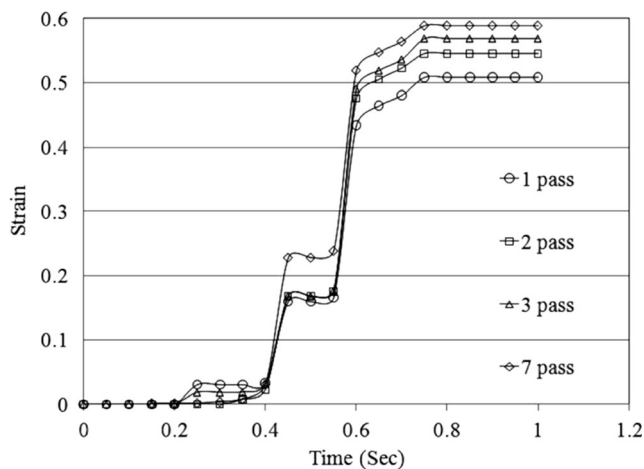


Fig. 12 Variation of plastic strain during deformation for passes #1, #2, #3 and #7

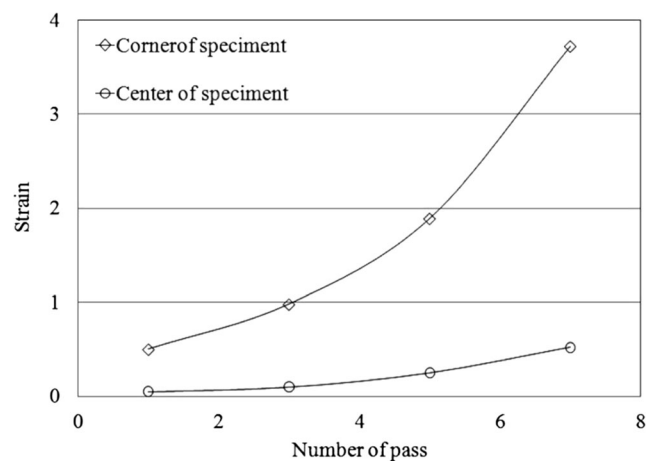


Fig. 14 Variation of plastic strain in multi-pass TE calculated from image analysis

Thus, the heterogeneity in strain distribution is decreased by increasing the number of passes.

- The corner regions of the sample experience higher strains than the center region, and also the heterogeneity in strain distribution increases by increasing the twist extrusion passes.

Compliance with ethical standards

Conflict of interest The authors declare that they have no conflict of interest.

References

- Valiev RZ, Estrin Y, Horita Z, Langdon TG, Zehetbauer MJ, Zhu YT (2006) Producing bulk ultrafine-grained materials by severe plastic deformation. *JOM* 58(4):33–39
- Smimova NA, Levit VI, Pilyugin VI, Kuznetsov RI, Davydova LS, Sazonova VA (1989) Evolution of structure of fcc single crystals during strong plastic deformation. *Phys Metals Metallogr* 61(6):127–134
- Segal MV, Reznikov VI, Drobysheskiy AE, Kopylov VI (1981) Plastic metal working by simple shear. *Izvestia Akademii nauk SSSR Metally* 1:115–123
- Salishchev GA, Valiakhmetov OR, Galeev RM (1993) Formation of sub micro crystalline structure in the titanium alloy VT8 and its influence on mechanical properties. *J Mater Sci* 28:2898–2903
- Saito Y, Utsunomiya H, Tsuji N, Sakai T (1999) Novel ultra-high straining process for bulk materials development of the accumulative roll-bonding (ARB) process. *Acta Mater* 47(2):579–583
- Huang JY, Zhu YT, Jiang HG, Lowe TC (2001) Microstructures and dislocation configurations in nanostructured Cu processed by repetitive corrugation and straightening. *Acta Mater* 49(9):1497–1505
- Varyukhin V, Beygelzimer Y, Kulagin R, Prokof'eva O, Reshetov A (2011) Twist extrusion: fundamentals and applications. *Mater Sci Forum* 667–669:31–37
- Beygelzimer Y, Reshetov A, Synkov S, Prokofeva O, Kulagin R (2009) Kinematics of metal flow during twist extrusion investigated with a new experimental method. *J Mater Process Technol* 209:3650–3656
- Abdul-Latif A, Dirras GF, Ramtani S, Hocini A (2009) A new concept for producing ultrafine-grained metallic structures via an intermediate strain rate: experiments and modeling. *Int J Mech Sci* 51:797–806
- Farbaniec L, Abdul-Latif A, Gubicza J, Dirras G (2012) Ultrafine-grained nickel refined by dislocation activities at intermediate strain rate impact: deformation microstructure and mechanical properties. *J Mater Sci* 47:7932–7938
- Dirras G, Chauveau T, Abdul-Latif A, Gubicza J, Ramtani S, Bui Q, Hegedus Z, Bacroix B (2012) Ultrafine-grained aluminum processed by a combination of hot isostatic pressing and dynamic plastic deformation: microstructure and mechanical properties. *Metall Mater Trans A* 43:1312–1322
- Akbari Mousavi SAA, Shahab AR, Mastoori M (2009) Computational study of Ti–6Al–4 V flow behaviors during the twist extrusion process. *Mater Des* 29:1316–1329
- Stolyarov VV, Beygelzimer Y, Orlov DV, Valiev RZ (2005) Refinement of microstructure and mechanical properties of titanium processed by twist extrusion and subsequent rolling. *Phys Metals Metall* 99(2):204–211
- Orlov D, Beygelzimer Y, Synkov S, Varyukhin V, Horita Z (2008) Evolution of microstructure and hardness in pure Al by twist extrusion. *Mater Trans* 49(1):6–10
- Orlov D, Beygelzimer Y (2009) Microstructure evolution in pure Al processed with twist extrusion. *Mater Trans* 50(1):96–100
- Mohammed Iqbal U, Senthil Kumar VS (2012) Experimental investigation and analysis of microstructure and mechanical properties on twist extrusion forming process of AA7075-T6 aluminum alloy. *Int J Mech Mater Eng (IJMME)* 7(1):24–30
- Mohammed Iqbal U, Senthil Kumar VS (2010) Experimental investigation on twist extrusion process of AA 6063 aluminum alloy. In: *Proceedings of the 3rd international and 24th all india manufacturing technology, design and research conference (AIMTDR)*, Vishakhapatnam, India, December 13–15
- Zendehdel H, Hassani A (2012) Influence of twist extrusion process on microstructure and mechanical properties of 6063 aluminum alloy. *Mater Des* 37:13–18
- Mohammed Iqbal U, Senthil Kumar VS (2013) Effect of process parameters on microstructure and mechanical properties on severe plastic deformation process of AA7075-T6 aluminum alloy. *Adv Mater Res* 622–623:705–709
- Ranjbar Bahadori S, Akbari Mousavi SAS (2012) The evolution of homogeneity in a transverse cross section of aluminum alloy profile deformed by twist extrusion. *JOM* 64:5
- Radim K, Miroslav G, Miroslav K, Ivo S, Adela M (2010) Twist channel angular pressing (TCAP) as a method for increasing the efficiency of SPD. *Mater Sci Eng A* 527:6386–6392
- Beygelzimer Y, Prilepo D, Kulagin R, Grishaev V, Abramova O, Varyukhin V, Kulakov M (2011) Planar twist extrusion versus twist extrusion. *J Mater Process Technol* 211:522–529
- Beygelzimer Y, Orlov D, Varyukhin V (2002) A new severe plastic deformation method: twist extrusion. In: *Ultrafine Grained Materials II*. Wiley, Hoboken, pp 297–304. doi:10.1002/9781118804537.ch35
- Beygelzimer Y (2005) Grain refinement versus voids accumulation during severe plastic deformations of polycrystals: mathematical simulation. *Mech Mater* 37:753–767
- Orlov D, Beygelzimer DY, Synkov S, Varyukhin V, Tsuji N, Horita Z (2009) Plastic flow, structure and mechanical properties in pure Al deformed by twist extrusion. *Mater Sci Eng A* 519(1–2):105–111
- Akbari Mousavi SA, Ranjbar Bahador S (2011) Investigation and numerical analysis of strain distribution in the twist extrusion of pure aluminium. *JOM* 63(2):69–76
- Kvačák T, Bidulská J, Kočíško R, Bidulský R (2011) Effect of severe plastic deformation on the properties and structural developments of high purity Al and Al-Cu-Mg-Zr aluminium alloy. In *Tech, Aluminium Alloys, Theory and Applications*, p 3–26
- Reshetov A, Korshunov A, Smolyakov A, Beygelzimer Y, Varyukhin V, Kaganova I, Morozov A (2011) Distribution of mechanical properties by volume in titanium billets processed by twist extrusion. *Mater Sci Forum* 667–669:851–856
- Nagasekhar AV, Yoon SC, Tick-Hon Y, Kim HS (2009) An experimental verification of the finite element modelling of equal channel angular pressing. *Comput Mater Sci* 46:347–351
- Latypov MI, Alexandrov IV, Beygelzimer YE, Lee S, Kim HS (2012) Finite element analysis of plastic deformation in twist extrusion. *Comput Mater Sci* 60:194–200
- Kulagin R, Latypov MI, Kim HS, Varyukhin V, Beygelzimer Y (2013) Cross flow during twist extrusion: theory, experiment, and application. *Metall Mater Trans A* 44:3211–3220